

X-Ray Diffraction Studies on Reverse-Annealed Polyethylenes

F. CSER,^{1*} J. L. HOPEWELL,¹ R. A. SHANKS²

¹ Cooperative Research Centre for Polymers, 32 Business Drive, Notting Hill, VIC 3168, Australia

² Department of Applied Chemistry, RMIT University, Melbourne, VIC 3000, Australia

Received 20 December 1999; accepted 3 June 2000

ABSTRACT: Linear low and high density polyethylene sheets were compression molded and crystallized at a 5–10°C/min cooling rate. Parts of the sheets were annealed at different temperatures up to 2°C below the melting temperature. The small angle X-ray scattering (SAXS) and the wide angle X-ray scattering intensities of the annealed samples were studied. SAXS intensities showed particle scattering with a bimodal size distribution. The estimated radii of gyration were 15–17 nm and 5–7 nm, respectively. The crystallinity and the radius of gyration increased slightly with increasing annealing temperature for some samples; others did not show any change. No peaks characteristic of intercorrelated lamellar crystallinity in the SAXS intensities developed during the annealing. The original broad peak of high density polyethylene disappeared from the SAXS recordings on annealing. The length of the perfect chain versus melting temperature was calculated by the Thomson-Gibbs formula and Flory's concept of melting temperature depression where methyl groups and tertiary carbon atoms at the branches were regarded as second components (solvent). Linear relationships were found for both cases. Experimental data for a linear low density polyethylene obtained from the literature were in between the two functions. A lamellar model of crystallization corresponding to the data is proposed. © 2001 John Wiley & Sons, Inc. *J Appl Polym Sci* 81: 340–349, 2001

Key words: polyethylene; annealing; X-ray diffraction; particle size; coupled system

INTRODUCTION

Several melting peaks can be produced in different grades of linear low density polyethylene (LLDPE) and low density polyethylene (LDPE) by stepwise isothermal crystallization.^{1–5} A thermal memory effect was first used to explain the phenomenon.^{1,2} The thermal memory effect could be

eliminated by a strain of 300–400%¹ or by a small increase in the temperature above the peak temperature of the individual melting endotherms (e.g., by 3 K). The change took place in the material in a time scale of 2–3 min.⁵

It was proposed by others^{6–9} that the multiple endotherm in the melting process was the result of some kind of fractionation of the material. The bases of this were the differences in the density of the branching along the polymeric chains. The smaller the unperturbed length of chain molecules between two branches, the lower the melting peak temperature of the endotherm.

Defoor and coworkers⁷ prepared bimodal blends of polyethylene (PE) and investigated

* Present address: RMIT University, Dept. of Chemical and Metallurgical Engineering, P.O. Box 2746V, Melbourne, VIC 3001, Australia.

Correspondence to: F. Cser.

Journal of Applied Polymer Science, Vol. 81, 340–349 (2001)
© 2001 John Wiley & Sons, Inc.

them both by differential scanning calorimetry (DSC) and small angle X-ray scattering (SAXS). Because their materials showed bimodal melting behavior, they expected double peaks in the SAXS curves, but only observed singular peaks. These peaks were obtained only after applying a Lorentz correction to the SAXS intensities [i.e., multiplying by $\sin^2(\Theta)$]. There were no peaks in the original SAXS recordings.

Balbontin and coworkers⁸ studied the distribution of the 1-butene units in LLDPE by different methods. Stepwise crystallization was applied using steps in the temperature of 10°C, and the unperturbed chain length was determined both from ¹³C-NMR and DSC data. The authors compared the lamellar thickness of the crystallites with the average length of the chain molecules between two branches in different fractions of the polymer, obtained by temperature rising elution fractionation. The lamellar thicknesses were calculated from the melting peak temperatures using the Thomson-Gibbs formula^{7,8}:

$$T_m = T_m^0 * \left(1 - \frac{2\sigma_e}{\Delta H * L} \right) \quad (1)$$

where T_m is the measured melting temperature, T_m^0 is the melting temperature of the crystals with infinite thickness (414 K), ΔH is the melting enthalpy of the crystals (279 J · cm⁻³ for PE), L is the thickness of the crystals, and σ_e is the surface energy of the crystals (8.7 μJ · cm⁻² for PE). The concept presumes that the melting is proceeding along the chain direction (**c**), i.e., the change in the crystallinity is proportional to the change in the thickness of the lamellae, only (see Fig. 1).

The average distance between two branches (unperturbed chain length) was calculated from the composition of the given fraction presuming a homogeneous distribution of the branches along the chains. One monomeric unit has a length of 2.53 Å, so the unperturbed chain length is calculated by multiplying the number of ethylene monomeric units between two branching by 2.53 Å. They found a reasonable agreement between the calculated distances and the lamellar thickness using two data sets.⁸

In our previous works,^{5,10} DSC and temperature-modulated DSC (TMDSC) data were presented that had been obtained on LDPE, LLDPE, high density polyethylene (HDPE), and isotactic polypropylene on samples crystallized by stepwise cooling using 3-K steps. Each step was fol-

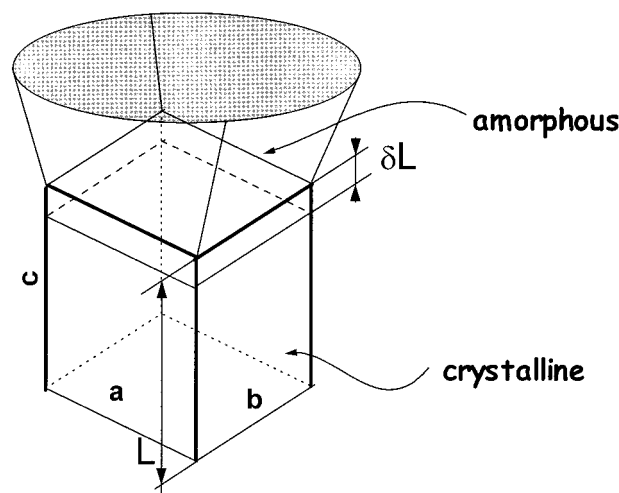


Figure 1 Melting of semicrystalline polymers according to the Thomson-Gibbs concept.

lowed by a 50-min isothermal period. The procedure is referred to as thermal fractionation (TF).

We found that the TF techniques produced multiple endotherms in polymers when branching or comonomers were present. HDPE and isotactic polypropylene did not show multiple peaks in the endotherm after TF. We also found a strong reversing heat flow during the melting process and this heat flow had multiple peaks also. Nevertheless, the reversibility of the melting decreased after TF.⁵ LLDPE produced using a metallocene catalyst also showed multiple peaks in the melting after TF.

TF samples have also been reverse annealed in a TMDSC.¹⁰ Reverse annealing means a series of heating/cooling cycles performed in TMDSC. The temperature of the samples was increased by a 2 K/min rate to 1 K below the peak temperature of the melting endotherm; then it was kept constant for 10 min. The sample was then cooled to 0°C at a 2 K/min cooling rate. This process was repeated according to the respective maxima found in the melting endotherm of the TF samples but the annealing temperature of the consecutive cycles was increased just under the maximum temperature of the next peak.

The heat capacities decreased to lower values during the annealing, which corresponded to that of the cooling cycle of the crystallized material when the annealing temperature was below that of the crystallization. In the other case, the heat capacities decreased to a value that was an extrapolation of the heat capacities of the crystallized material to higher temperatures. We found

that the heat capacities reached their minimum value within 1–3 min. The peak temperature of the next maximum in the endotherm increased by 2 K with respect to the same peak measured during a simple melting cycle.¹⁰ The endotherm peak at the highest temperature was also shifted by 2–3 K to higher values with respect to its original position in the TF sample. It is generally accepted that this shift is the result of an increase of the lamellar thickness of the crystallites.¹¹ This change should influence the SAXS intensities of the material. The aim of this work was to show the effect of the annealing of the PEs on the SAXS intensities.

Semicrystalline polymers are generally regarded as periodic systems where consecutive layers of the lamellar crystallites and the amorphous phases form a periodic structural system. A diffraction peak is expected for these systems. The distance of periodicity (d) can be calculated from the peak of the maximum of the X-ray intensities using the Bragg equation :

$$d = \frac{2 \sin(\theta)}{\lambda} \quad (2)$$

where Θ is the half of the diffraction angle of the peak and λ is the wavelength of the X-ray. This formula is generally applied to calculate the length of periodic systems (Bragg periodicity). The structure is supposed to have crystalline lamellas with a fairly homogeneous thickness and separated by an amorphous phase with also a fairly homogeneous layer thickness. The lamellar thickness of the crystals is generally calculated from the Bragg periodicity modified by the degree of crystallinity of the system. This latter was determined from wide angle X-ray diffraction (WAXS), DSC, or density measurements (see, e.g., Dlugosz et al.¹²

There is another concept of the origin of the SAXS intensities—the particle scattering principle. The structural basis of this scattering is a dispersion of one phase in the other one where the two phases have different electron densities.¹³ The scattering intensities are functions of the difference in the electron densities between the matrix and the dispersed particles, the volume concentration of the particles as well as their radii of gyration. This scattering has a maximum at zero angle with a Gaussian shape of the scattering toward greater angles. The $\log(I)$ versus square of the scattering vector s ($s = 2\pi/d$) results in a slope

of the Gaussian scattering curve and this slope can be used to determine the dimension (radius of gyration) of the scattering particle [differential form of the Guinier approximation; see eq. (3)].

$$\frac{d \ln(I)}{ds^2} = 3 * R_G^2 \quad (3)$$

where R_G is the radius of gyration of the scattering particle. From the radius of gyration, the thickness of a lamella with infinite lateral extension can be obtained with a multiplication by $12^{1/2}$ (3.464. . .).

A multiplication factor has been used to modify SAXS intensity data of semicrystalline polymers in some of the relevant literature^{12,15–17} since the early seventies. This means that the intensities are generally multiplied by a factor of $\sin^2(\Theta)$ (in practical calculations by s^2). This kind of correction is called the Lorentz correction. The Lorentz factor is used in the structure factor calculation of reciprocal lattice systems¹⁴ (single crystals) and means a multiplication by a factor proportional to $\sin(2\Theta)$.

The use of this factor for semicrystalline polymers may be severely criticized because the factor produces an artificial peak in the intensities and might be completely misleading in the interpretation of the data.^{12,18} It can, but should not, be used to correct the position of the peaks of the reciprocal lattice diffraction. If there are also particles in the periodical system, particle scattering will be superimposed on the scattering caused by reciprocal lattice and a Lorentz correction will destroy the shape of the curve, such that it cannot be used for calculations. The sum of the intensities originating from the particle scattering might shift the position of the peak derived from the reciprocal lattice and its position will also be incorrect. Therefore, the two scattering types must be separated from each other and handled individually.

In our recent research, the SAXS curves of many PEs, polypropylenes, and their blends, did not show any definite maximum indicating the dominance or even the presence of a reciprocal lattice type of scattering. Therefore, the Lorentz correction was abandoned and the system was handled as if it consisted of particles dispersed in a matrix.

EXPERIMENTAL

Materials

All of the materials are industrial products and were prepared by the Ziegler/Natta process. Their

Table I The Type, Density, and the Melt Flow Index of the Materials Used

Material	Medium of the Polymerization	Comonomer	Density (kg · m ⁻³)	MFI (g/10 min)
C8-LLDPE1	Solution	Octene	923	0.94
C8-LLDPE2	Solution	Octene	923	1.10
C6-LLDPE	Gas phase	Hexane	922	0.78
C4-LLDPE	Gas phase	Butene	918	1.00
HDPE	Gas Phase	—	NA	0.20

main characteristics are given in Table I. C8-LLDPE1 has 1.25 m % of octene as comonomer. $M_w = 124,600$, $M_n = 33,200$, and the polydispersity is 3.75. The composition and the molecular weight for C8-LLDPE2 are not given, but they should be nearly the same as for C8-LLDPE1. C6-LLDPE has 2.3 m % hexane as comonomer. Its molecular weight is not given. Neither the comonomer content, nor the molecular weight data are given for C4-LLDPE. These latter polymers should have higher polydispersity than the C8-LLDPEs, as they showed sharper melting endothermic peak with a much broader secondary crystallization.¹⁰

Sample Preparation

The pellets were compression molded at 150°C using 150-MPa pressure to form sheets of 2-mm thickness. The sheets were crystallized within the die using water cooling. The approximate cooling rate at the crystallization was 5–10°C/min.

Smaller portions of the sheets were heated and annealed for 60 min at various temperatures in an oven with a well-regulated temperature control. The program for LLDPEs started at 94°C, then with heating increments of 4°C. The maximum annealing temperature was 122°C. This is 3–4°C below the peak temperature of the materials determined by TMDSC using a 2 K/min heating rate on samples cooled from the melt by a 2 K/min cooling rate (standard state). The samples annealed for 60 min were then cooled to room temperature at a slow cooling rate ($\ll 2$ K/min) by wrapping the samples in heat isolating foam. HDPE was annealed at temperatures started from 112 up to 132°C. The latter temperature was too high and the sample melted partially.

X-Ray Diffractometry

A Rigaku Geigerflex generator was used with a wide angle and a Kratki type small angle goniom-

eter. A 30-kV accelerating voltage and a 30-mA current was applied for producing Ni-filtered Cu-K α radiation.

Wide angle X-ray intensities were collected from $2\Theta = 3$ to 50° with steps of 0.05° using transmission techniques on the compression molded samples with 2-mm thickness. Data were collected and processed using separate graphics software.

Small angle X-ray intensities were collected from $2\Theta = -1$ to 1° in steps of 0.002° using the same samples as for wide angle X-ray. Background intensities were collected for each type of sample (thickness, absorption) from a master sample positioned just in front of the counter. Data were collected and processed using a computer program for removing the background and calculating the average of the data from the two sides of the primary beam. The maximum resolution of the SAXS camera was 120 nm as the intensities could generally be collected up to $2\Theta = 0.06^\circ$. Slit correction was applied using smooth derivation of the raw data (five data points, second order approach) and a numerical integration. As the SAXS intensities showed particle type of scattering,¹³ Lorentz correction¹⁴ was not applied.

The peak melting temperature of the samples was determined from the total heat flow curves obtained by a TMDSC, using a TA Instruments 2920 MDSC.¹⁹ An intercooler device was used to produce the cooling power. Helium was used as the purge gas with a flow rate of 25 mL/min. Heating and cooling rates of 2 K/min were applied with a 0.6-K modulation amplitude and 40-s modulation period. This is a medium type of modulation (cooling during the heating).²⁰ The calorimetric data are collected in Table II.

RESULTS

Figures 2 and 3 show the WAXS intensities versus scattering angle for C6-LLDPE and HDPE,

Table II Peak Melting Temperature and Melting Enthalpy Obtained from the Total Heat Flow Curves, Crystallinity from Melting Enthalpy after Annealing and Crystallinity from Density of the PE Samples

	C4-LLDPE	C6-LLDPE	C8-LLDPE1	C8-LLDPE2	HDPE
Annealing at (°C)	122	122	122	122	128
T_m (°C)	127.46	127.69	127.07	127.38	132.29
ΔH_m [J/g]	114.75	139.4	136.7	140.6	202.4
Crystallinity (DSC) (%)	39.6	48.1	47.1	48.5	69.8
Crystallinity (dens.) (%)	43.9	46.5	47.1	47.1	NA
L1 (X-ray) (nm)	52	41	52	56	50
L2 (X-ray) (nm)	19	21	20	17	17
L (caloric) (nm)	18	18	18	18	29

respectively. There are very small changes in the WAXS intensities, if they are there at all, as the differences approach the reproducibility of the WAXS measurements.

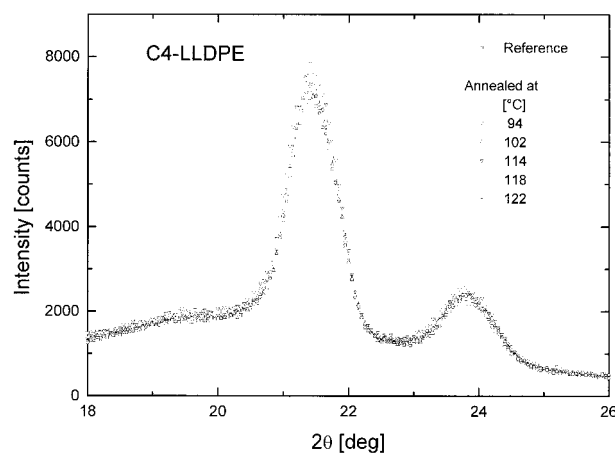
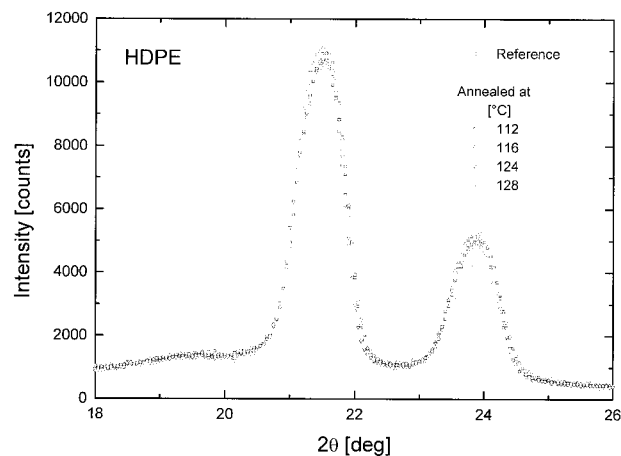
There is no remarkable change in the crystallinity of the samples during the annealing. This supports our previous result obtained by TMDSC.¹⁰ Nevertheless, there are some changes in the heat flow curves of the samples caused by the annealing, but this does not influence either the overall crystallinity or the particle size of the crystals at all. The greatest change can be seen for samples that have been annealed at a temperature just below the melting temperature. There is one broad melting peak below the annealing temperature and a sharp, strong one corresponding to the melting. The ratio of the sharp second melting peak with respect to the broad one is approximately 1:3.¹⁰

According to the concept of folded chain lamellar crystallization, the extension of the crystalline

lamellae with respect to their thickness is great. Particle size of the crystals along the direction of [110] and [200] can be calculated from the half width of the diffraction peak using the Scherrer formula²¹ [see eq. (4)]:

$$L = \frac{K * \lambda}{d * B * \cos(\Theta)} \quad (4)$$

where L is the particle size expressed in the scale of λ , d is the Bragg periodicity corresponding to the peak, B is the half width of the peak expressed in radians, and K is a constant with a value of 1.07. The particle size calculated from the line width of the diffraction peaks shown in Figures 2 and 3 [(110) and (200)] is 6.5 nm. This means that the unperturbed lateral dimension of the lamellae is small. Kavesh and Schultz²² suggested that this smaller particle size of the lamellae is the

**Figure 2** WAXS intensities of the C4-LLDPE after annealing at different temperatures.**Figure 3** WAXS intensities of the HDPE after annealing at different temperatures.

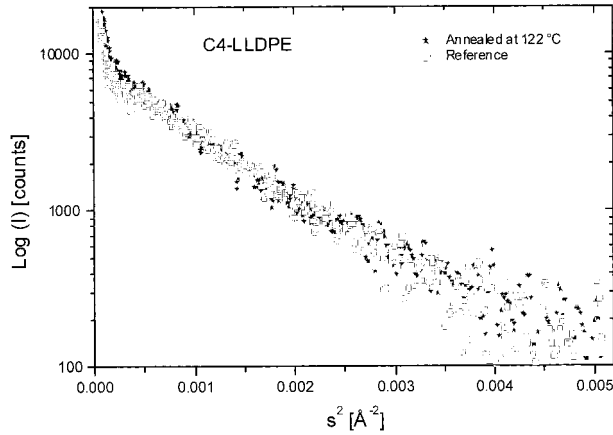


Figure 4 Guinier representation of the SAXS intensities of the C4-LLDPE annealed at 122°C for 1 h and of its reference.

result of distortions within a physically much bigger lamella.

The lamellar thickness is supposed to be obtained from the SAXS intensities. Figures 4–8 show the SAXS intensities of the different PEs as the function of their annealing temperature in a Guinier representation. Because the changes are very small, most of the Figures show only the SAXS intensities of the samples annealed at the highest temperature in comparison with those of the reference samples.

C4-LLDPE and C6-LLDPE do not have any peaks in SAXS intensities, as can be seen in Figures 4 and 5. They show two intercepting straight lines, the slope of which change slightly (C4-LLDPE) or not at all (C6-LLDPE) after annealing. The radii of

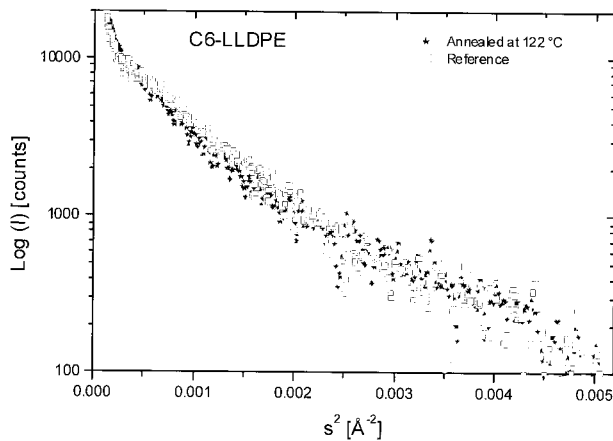


Figure 5 Guinier representation of the SAXS intensities of the C6-LLDPE annealed at 122°C for 1 h and of its reference.

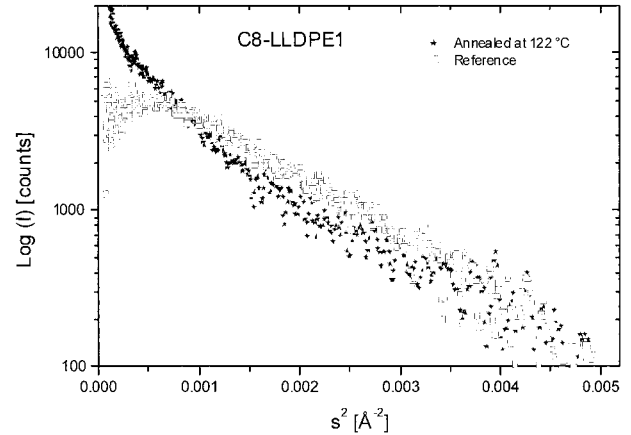


Figure 6 Guinier representation of the SAXS intensities of the C8-LLDPE1 annealed at 122°C for 1 h and of its reference.

gyration for the particle sizes corresponding to the straight lines of C4-LLDPE are 15.0 nm and 5.6 nm (52 and 19 nm); those for C6-LLDPE are 11.8 nm and 6.1 nm (41 and 21 nm). The figures in parentheses are the corresponding lamellar thicknesses.

C8-LLDPEs show initially a broad peak superimposed on a straight line as it is shown in Figures 6 and 7. The intensities at higher angles than that of the peak decrease with increasing annealing temperature; those with smaller angles increasing with decreasing angles and form a straight line at the highest annealing temperatures. The change is particularly great for C8-LLDPE1. The radii of gyration for C8-LLDPE1 are 14.8, 5.03 (52 and 20 nm); those for C8-

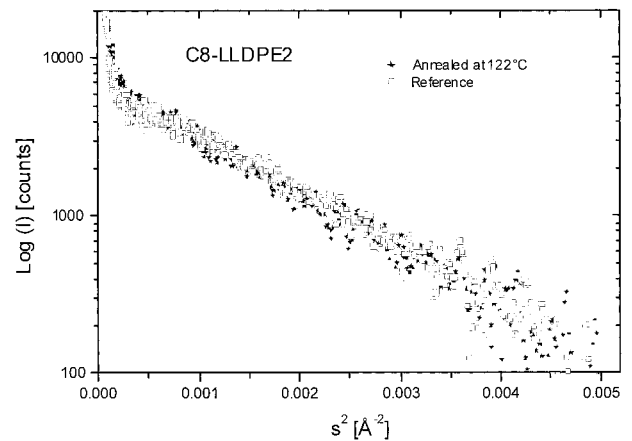


Figure 7 Guinier representation of the SAXS intensities of the C8-LLDPE2 annealed at 122°C for 1 h and of its reference.

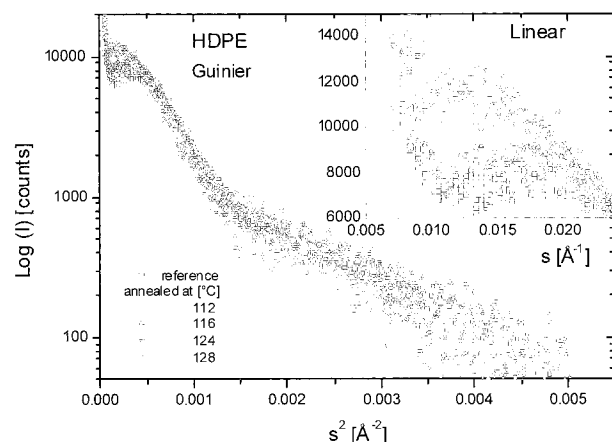


Figure 8 Guinier representation of the SAXS intensities of HDPE during annealing at different temperatures.

LLDPE2 are 16.2 and 5.05 nm (56 and 17 nm), respectively.

Because all of these LLDPEs have a melting peak temperature after annealing at 127°C, their maximal lamellar thickness calculated by the Thomson-Gibbs formula is 18 nm. This value corresponds to the second, i.e., to the smallest value, which can be obtained from the Guinier interpretation of the SAXS intensities (see Table II).

HDPE has a definite peak in the SAXS intensities of the reference sample, which is evident in the I versus s representation in Figure 8. Here, we show the SAXS intensities of all of the annealed samples. Using the Lorentz correction, two broad peaks formed with maxima corresponding to periodicities of 26 nm and 13 nm, respectively.¹⁸ These maximums can be accepted as first- and second-order Bragg reflections of a reciprocal lattice. From the “line width,” however, the particle sizes of the periodicity are 75 and 46 nm. The corresponding numbers of lamellas in the crystalline particles are 2.9 and 3.5. These are very small numbers. They mean there is no true reciprocal lattice and consequently no intercorrelated lamellar structure in the system. Therefore, the peaks formed after the Lorentz correction in the SAXS intensities are artefacts.¹⁸

Samples with increasing annealing temperature show increasing scattering intensities at lower angles (below the peak) and decreasing ones at higher angles (above the peak). The sample annealed at 128°C, just below the melting temperature, definitively shows a particle type of scattering with bimodal particle size distribution and it shows practically no peak (Fig. 9). The

straight line at lower angles corresponds to a radius of gyration of 14.4 nm; that at the greater angles to 4.9 nm. These values represent lamellar thicknesses of 50 and 17 nm. Figure 9 also shows the SAXS intensities of the reference sample for comparison. This sample shows particles with a radius of gyration of 5.0 nm, corresponding to a lamellar thickness of 17.3 nm.

From the peak melting temperature, a 29-nm lamellar thickness could be calculated using the Thomson-Gibbs formula. This value corresponds to the larger lamellar size obtained from the Guinier representation of the SAXS intensities (see Table II).

The change of the SAXS intensities toward those without peaks is completely unexpected. If we would have some lamellar structure, particularly with a degree of crystallinity higher than 50% as is the case for HDPE, where it is 70%, the annealing should improve its packing. As a consequence, a structure with stronger periodicity is expected that should result in a sharper, and consequently, in a greater peak based on SAXS intensities. This is not the case. The diffraction “peak” that was originally present in the diffractogram actually strongly reduced during the heat treatment.

Naturally, a peak can be produced by the application of a Lorentz correction as is the case in many articles.^{15–17} The intensity curve of HDPE was analyzed previously,¹⁸ and three components were fitted to the curve. Two of them were functions of the particle scattering and one was reciprocal lattice scattering. The integral values showed that the reciprocal lattice component

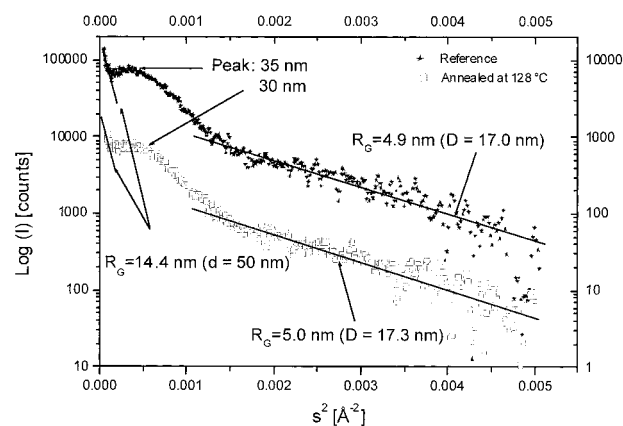


Figure 9 Guinier representation of the SAXS intensities of the HDPE annealed at 128°C and of its reference.

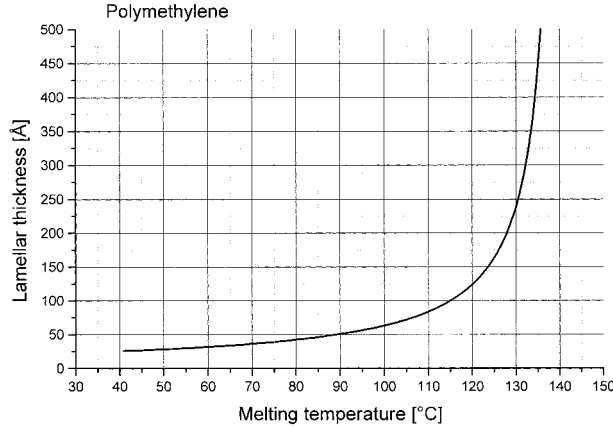


Figure 10 Lamellar thickness versus melting temperature calculated by the Thomson-Gibbs relation.

might not exceed 10% in its volume. The mode of scattering was predominantly particle scattering. It can be seen that the reciprocal lattice scattering is decreased and has nearly been vanished by increasing the temperature of the annealing.

DISCUSSION

The original expectations of the study were to get definite periodicity with increased length by an increased temperature of annealing. Instead of our expectations, we have received either no changes in a purely particle type of scattering (C6-LLDPE) or an even smaller extent of periodicity (HDPE) than without annealing. The particle type of the scattering was enhanced; nevertheless, it was expected to be reduced.

Table II contains the peak melting temperatures of the polymers annealed just below the melting temperature and the corresponding thickness of the crystalline lamellae as estimated by the Thomson-Gibbs formula. According to eq. (2) we can construct a graph representing the lamellar thickness as a function of the peak melting temperature (Fig. 10).

It has been shown¹⁸ that the lamellar thickness calculated from the X-ray data, and those calculated by this formula are not comparable. This is also the case in this research. LLDPE showed a very similar melting peak temperature and similar SAXS intensities before and after annealing. In contrast, HDPE had a much higher melting peak temperature after annealing, but its SAXS intensities after annealing did not differ markedly from those of the LLDPEs. This is nat-

urally a contradiction. Balbotin et al.⁸ also concluded that the X-ray lamellar thickness does not correlate with the values obtained from the melting peak temperature.

There is another way to calculate the melting temperature of semicrystalline polymers containing comonomers, proposed by Flory.²³ LDPE and LLDPE are copolymers. If we regard the branching points as well as the end groups of the polymeric chains as if they were another chemical component with respect to the elements of the main chain, we have a two-component thermodynamic system. One of the components is formed from the monomeric units of the main chain, which is called in our case polymethylene. The other one is formed from all of the atomic groups, which are different from the elements of the perfect segments. The peak melting temperature can be regarded as the end temperature of the solution of the perfect crystalline elements in the other component, as solvent. Equation (5) describes the change of the peak melting temperature as a function of the concentration of the solvent (with indices 1):

$$\frac{1}{T_m} - \frac{1}{T_m^0} = \frac{R}{\Delta H_u} \frac{V_u}{V_1} (\Phi_1 - \chi\Phi_1^2) \quad (5)$$

where T_m is the peak melting temperature, T_m^0 is 414 K for PE, R is the universal gas constant, ΔH_u is the melting enthalpy of the solute, V_1 and V_u are the molecular volume of the solvent and the solute, χ is the interaction parameter, and Φ_1 is the volume fraction of the solvent. This means that the polymeric system is handled as would be a two-component thermodynamic system. The components, however, are coupled by chemical bonds. This kind of description was previously proposed to describe the transition and melting temperatures of liquid crystalline materials as a function of the mol fraction of the soft segments with respect to the hard segments.²⁴

The change of the melting temperature can be expressed now with the mol fraction of the unperturbed chain length (x_u) in the following form²³:

$$\frac{\Delta T}{T_m^0} \approx T_m \frac{R}{\Delta H_u} \ln x_u \quad (6)$$

Equation 1 can also be transformed to a similar form :

$$\frac{\Delta T}{T_m^0} = \frac{2\sigma_c}{\Delta H_u} \frac{1}{L} \quad (7)$$

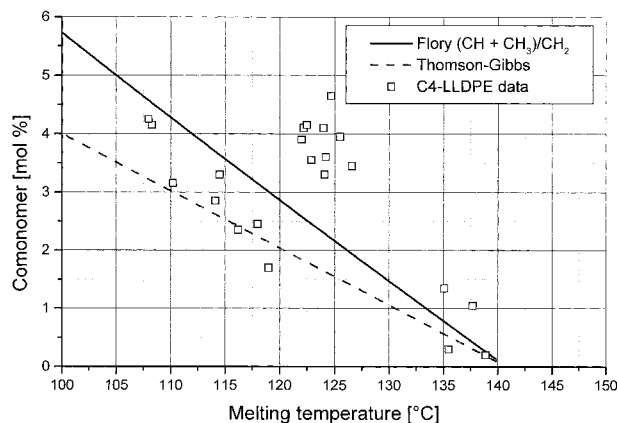


Figure 11 Comonomer content versus melting temperature of PEs.

The two equations have identical form. One describes the effect of the lamellar thickness on the melting temperature; the other describes that of the solvent that is actually coupled to the crystalline solute. It is utilized in this transformation, that when $x_u \approx 1$, then $\ln(x_u) \approx x_u$.

The lamellar thickness can be related to the number of the carbon atoms in the perfect crystalline chains as the periodicity along the chain axes is 2.53 \AA and so $x_u = 2.35/L$. The concentration of the perfect chain elements can also be related to the number of perfect chain elements and through this to lamellar thickness. Both functions are shown in Figure 11 as a function of the peak melting temperature. The two functions form two straight lines with similar but different slopes. Figure 11 also shows the peak melting temperature versus the length of the unperturbed molecular segments data expressed as a mol fraction by Balbotin et al.⁸ obtained on C4-LLDPE. These data equally fit both functions because they are mainly distributed in between.

Peticolas et al.²⁵ and Dlugosz et al.¹² were dealing with the correlation of the fold length determined by low-frequency Raman spectra and by SAXS. Both found smaller length by Raman than by SAXS. The lamellar thickness was even smaller when a Lorentz correction was applied. Dlugosz et al.¹² also showed a transmission electron micrograph pattern of chlorosulfonic acid-treated PE with smaller periodicity than had been expected from Raman measurements. The authors tried to explain their result by the tilting of the polymeric chains. The problem is that their observed periodicity does not mean lamellar thickness of the crystals; it also contains the

thickness of the amorphous phase. This means that the correlation between the lamellar thickness measured by different methods is wrong. They found better correlation when they used a mat of single crystals grown from dilute solution. Really, in this case there are also higher order diffraction peaks in the SAXS intensity curve [(002), (003), etc.] as has also been shown by Wang and Harrison.²⁶ We believe that the root of the problem is in the difference in the mode of the crystallization. Crystals grown from dilute solution show intercorrelated periodic systems, but crystals grown from the bulk show particle-type systems. A possible representation of this model is shown in Figure 12.

The main characteristic of the bulk-crystallized samples is that the crystals do not have a definite, plane-parallel shape. In other words, the parallel-arranged chain elements do not end at a definite plane. The chains of the crystals continue into the amorphous phase and through the amorphous phase they pass into the next crystallite or return to the same lamella in an irregular way. Naturally, the branching segments and the chain ends are in the amorphous phase, as the branching cannot be incorporated into the crystals. (The chain ends can be incorporated, but they would cause severe distortions; therefore, their incorporation is energetically unfavorable.) The crystalline lamellae are not arranged parallel because they do not correlate with each other. A plane parallel (epipedon) shape of crystallites would be forced to be arranged parallel and to form periodic structures. This is not the case.

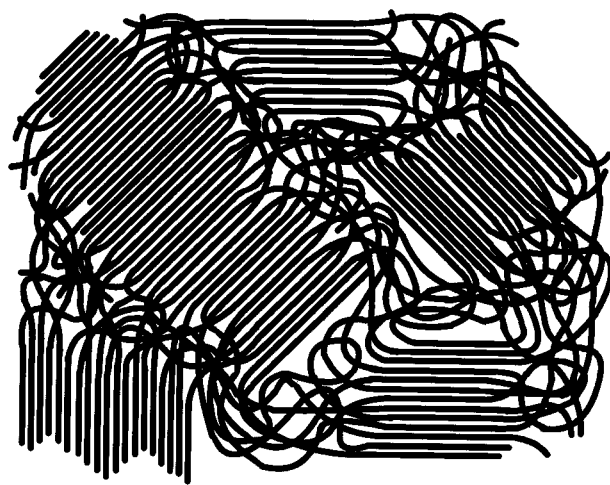


Figure 12 The proposed structural model of semicrystalline polymers. The amorphous phase is coupled to the crystalline phase by chemical bond at the end of the molecular chains forming the crystals.

Because the amorphous phase is chemically bound to the crystalline phase, the two thermodynamic systems are not isolated; they are coupled. The consequence is that in the heating cycle of the annealing, the thickness of the crystalline region decreases with increasing temperature without material transport through a surface. At the annealing temperature, the heat capacities are reduced to a lower value in a rapid process indicating changes in the liquid (amorphous) phase.

CONCLUSIONS

The reversed annealing experiments together with the result in reversible melting studies showed that the structural relationships in semicrystalline polymers should be reconsidered. The generally accepted folded chain lamellar model describes the properties of the polymeric single crystals formed from diluted solutions. This model does not describe satisfactorily the structure of bulk-crystallized polymers. The coupled two-phase thermodynamic system might be used to characterize the caloric behavior of the bulk-crystallized semicrystalline polymers. Further theoretical work should be performed to have a proper thermodynamic description of this kind of system.

The authors are indebted to Ms. K. Tajne for her participation in the experimental work.

REFERENCES

- Varga, J.; Menczel, J.; Solti, A. *J Therm Anal* 1979, 17, 333.
- Varga, J.; Toth, E. *Makromol Chem Macromol Symp* 1986, 5, 213.
- Addison, E.; Ribeiro, M.; Fontanille, M. *Polymer* 1992, 33, 4337.
- Wolf, B.; Kenig, S.; Klopstock, J.; Miltz, J. *J Appl Polym Sci* 1996, 62, 1339.
- Cser, F.; Hopewell, J. L.; Shanks, R. A. *J Therm Anal* 1998, 54, 707.
- Wild, L.; Chang, S.; Shankernarayanan, M. J. *Polym Prepr* 1990, 31, 270.
- Defoor, F.; Groeninckx, G.; Raynaers, H.; Schouterden, P.; Van Der Heiden, B. *J Appl Polym Sci* 1993, 47, 1839.
- Balbontin, G.; Camurati, I.; Dall Occo, T.; Finotti, A.; Franzese, R.; Vecellio, G. *Angew Makromol Chem* 1994, 219, 139.
- Zhou, H.; Wilkes, G. L. *Polymer* 1997, 38, 5735.
- Cser, F.; Hopewell, J. L.; Tajne, K.; Shanks, R. A. *J Therm Anal*, to appear.
- Wunderlich, B. *Macromolecular Physics*; Academic Press: New York, 1976; Vol. 2.
- Dlugosz, J.; Fraser, G. V.; Grubb, D.; Keller, A.; Odell, J. A.; Goggin, L. *Polymer* 1976, B17, 471.
- Glatzer, O.; Kratky, O. *Small Angle X-ray Scattering*; Academic Press: London, 1982.
- Bunn, C. W. *Chemical Crystallography*, 2nd ed.; Clarendon Press: Oxford, 1961.
- Russel, T. P.; Koberstein, J. T. *J Polym Sci Polym Phys Ed* 1985, 23, 1109.
- Butler, M. F.; Donald, A. M.; Ryan, A. J. *Polymer* 1997, 38, 5521.
- Ryan, A. J.; Brass, W.; Mant, G. R.; Derbyshire, G. E. *Polymer* 1994, 35, 4537.
- Cser, F. *J Appl Polym Sci*, to appear.
- Reading, M.; Elliott, D.; Hill, V. L. *J Therm Anal* 1993, 40, 949.
- Cser, F.; Rasoul, F.; Kosior, E. *J Therm Anal* 1997, 50, 727.
- Lipson, H.; Steeppe, H. *Introduction to X-Ray Powder Diffraction Patterns*; McMillan: London, 1970; p. 246.
- Kavesh, S.; Schultz, J. M. *J Polym Sci Part A* 1970, 8, 243.
- Flory, P. J. *Principles of Polymer Chemistry*; Cornell University Press: Ithaca, NY, 1953; p. 569.
- Cser, F. *Mater Forum* 1990, 14, 81.
- Peticolas, W. L.; Hibler, G. W.; Lippert, J. L.; Peterlin, A.; Olf, H. *Appl Phys Lett* 1971, 18, 87.
- Wang, J.-I.; Harrison, I. R. *J Appl Crystallogr* 1978, 11, 525.